5 Multiplets in Transition-Metal Ions and Introduction to Multiband Hubbard Models

Robert Eder
Institut für Festkörperphysik
Karlsruhe Institute of Technology

Contents

1   Introduction

Compounds containing $3d$ transition-metal ions have been intriguing solid state physicists ever since the appearance of solid state physics as a field of research. In fact, already in the 1930's NiO became the first known example of a correlated insulator in that it was cited by deBoer and Verwey as a counterexample to the then newly invented Bloch theory of electron bands in solids [1]. During the last 25 years $3d$ transition-metal compounds have become one of the central fields of solid state physics following the discovery of the cuprate superconductors, the colossal magnetoresistance phenomenon in the manganites and, most recently, the iron-pnictide superconductors.

It was conjectured early on that the reason for the special behavior of these compounds is the strong Coulomb interaction between electrons in their partially filled $3d$-shells. The $3d$ wave functions are orthogonal to those of the inner-shells — such as $1s$, $2s$, $2p$, $3s$ and $3p$ — solely due to their angular part $Y_{2,m}(\vartheta, \varphi)$. Their radial part $R_{3,2}(r)$ therefore is not pushed out to regions far from the nucleus by the requirement to be orthogonal to the inner shell wave functions and therefore is concentrated close to the nucleus (the situation is exactly the same for the $4f$ wave functions). Any two electrons in the $3d$-shell thus are forced to be close to each other on average so that their mutual Coulomb repulsion is strong (the Coulomb repulsion between two $3d$ electrons is small, however, when compared to the Coulomb force due to the nucleus and the inner shells so that the electrons *have to* stay close to one another!). For clarity we also mention that the Coulomb repulsion between two electrons in the inner shells of most heavier elements is of course much stronger than between $3d$ electrons. This, however, is irrelevant because these inner shells are several 100–1000 eV below the Fermi energy so that they are simply completely filled and inert. On the other hand, the $3d$-orbitals in transition-metal compounds or the $4f$-orbitals in materials containing the Rare Earth elements participate in the bands at the Fermi level so that the strong Coulomb interaction in these orbitals directly influences the conduction electrons. The conduction bands in such compounds therefore form dense many-body-systems of strongly interacting electrons and the energy from the Coulomb repulsion is large compared to the average kinetic energy. This dominance of the interaction energy in turn implies a propensity to show ordering phenomena and the ensuing phase transitions. It is therefore ultimately the Coulomb repulsion in the partially filled $3d$-shells of the transition-metals and the $4f$-shells of the rare earths which gives rise to the wide variety of spectacular phenomena observed in these compounds. Let us therefore discuss this Coulomb interaction in more detail.

2   Multiplets of a free ion

2.1   General considerations

As an example let us consider an Ni^{2+} ion in vacuum which has the electron configuration [Ar] $3d^8$. It is a standard exercise in textbooks of atomic physics to show that the d^8 configuration, which is equivalent to d^2, has the following multiplets or terms: ^3F, ^3P, ^1G, ^1D and ^1S,

Term	J	E (eV)
^3F	4	0.000
	3	0.169
	2	0.281
^1D	2	1.740
^3P	2	2.066
	1	2.105
	0	2.137
^1G	4	2.865
^1S	0	6.514

Table 1: *Energies of the multiplets of Ni^{2+} (taken from Ref. [2]. J is the total angular momentum quantum number and the $J = 4$ member of ^3F has been taken as the zero of energy.*

whereby according to the first two Hund's rules ^3F is the ground state. 'Multiplets' thereby is simply another word for 'eigenstates of the system of 26 electrons in the electric field of the Ni nucleus' (the nuclear charge of Ni is 28). Actually, the electrons in the shells below the $3d$-shell may be considered as inert due to the large binding energies of these shells so that to very good accuracy one can consider only the 8 electrons in the $3d$-shell. The energies of the multiplets can be deduced experimentally by analyzing the optical spectrum of Ni vapor and are listed in Table 1. They span a range of several eV whereby multiplets with nonzero spin are in addition split by spin-orbit coupling which results in intervals of order 0.1 eV. All of these eigenstates correspond to the same electron configuration, namely [Ar] $3d^8$, so that the fact that, say, ^3P has a higher energy than ^3F is not due to an electron having been promoted from a state with low energy to one with high energy as in an optical transition. Rather, the excited multiplets – ^3P, ^1G, ^1D and ^1S – should be viewed as collective excitations of the 8-electron system, similar in nature to a plasmon in an electron gas. And just as a plasmon can exist only due to the Coulomb interaction between electrons, the multiplet splitting in atomic shells also originates from the Coulomb interaction between electrons. To understand it we therefore need to discuss the Coulomb interaction between electrons in a partially filled atomic shell.

As a first step we introduce Fermionic creation and annihilation operators $c^\dagger_{n,l,m,\sigma}$ which create an electron with z-component of spin σ in the orbital with principal quantum number n, orbital angular momentum l, and z-component of orbital angular momentum m. In the case of a partly filled $3d$-shell all $n_i = 3$ and all $l_i = 2$ identically, so that these two indices could be omitted, but we will keep them for the sake of later generalizations. In the following we will often contract (n, l, m, σ) to the compound index ν for brevity, so that, e.g., $c^\dagger_{\nu_i} = c^\dagger_{n_i,l_i,m_i,\sigma_i}$.

The procedure we will follow is degenerate first-order perturbation theory as discussed in practically any textbook of quantum mechanics. The unperturbed Hamiltonian H_0 thereby corresponds to the energies of the different atomic shells

$$H_0 = \sum_{n,l} \epsilon_{n,l} \sum_{m,\sigma} c^\dagger_{n,l,m,\sigma} c_{n,l,m,\sigma}$$
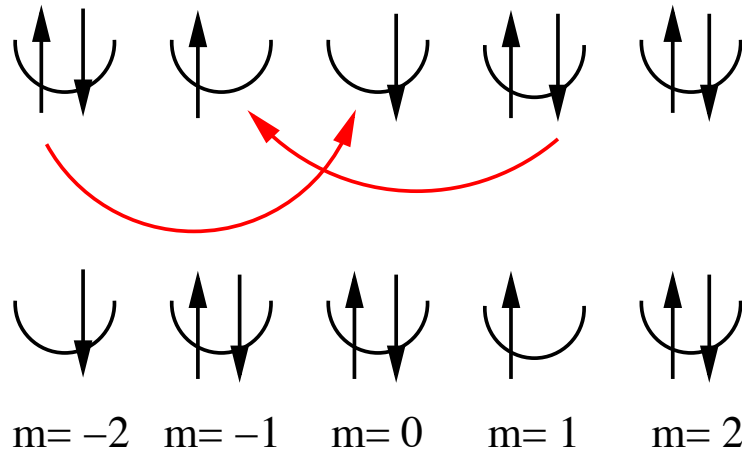
Fig. 1: *Coulomb scattering of two electrons in the d-shell. In the initial state $|\nu\rangle$ (top) the electrons are distributed over the five d-orbitals which are labeled by their m-values. Due to their Coulomb interaction two electrons scatter from each other and are simultaneously transferred to different orbitals, resulting in the state $|\mu\rangle$ (bottom).*

whereas the Coulomb interaction is considered as the perturbation H_1. The d^n configuration comprises all states which are obtained by distributing the n electrons over the $2 \cdot 5 = 10$ spin-orbitals:

$$|\nu\rangle = |\nu_1, \nu_2 \ldots \nu_n\rangle = c_{\nu_1}^\dagger c_{\nu_2}^\dagger \ldots c_{\nu_n}^\dagger |0\rangle \ . \tag{1}$$

and the number of these states obviously is $n_c = 10!/(n! \, (10-n)!)$. In writing the basis states as in (1) we need to specify an ordering convention for the creation operators on the right hand side. For example, only states are taken into account where $m_1 \leq m_2 \leq m_3 \cdots \leq m_n$. Moreover, if two m_i are equal the $c_{m_i\downarrow}^\dagger$-operator is assumed to be to the left of the $c_{m_i\uparrow}^\dagger$-operator. If we adopt this convention, every possible state obtained by distributing the n electrons over the 10 spin-orbitals is included exactly once in the basis. If the n_i and l_i were to take different values we could generalize this by demanding that the (n_i, l_i, m_i)-triples be ordered lexicographically. As will be seen below, strict application of an ordering convention for the Fermi operators is necessary to determine the correct Fermi signs for the matrix elements.

If only H_0 were present all the states (1) would be degenerate. The Coulomb interaction H_1 between the electrons then (partially) lifts this degeneracy and this is the physical reason for the multiplet splitting. The standard procedure in this a situation is to set up the matrix $h_{\mu,\nu} = \langle\mu|H_1|\nu\rangle$ and diagonalize it to obtain the first order energies and wave functions [3]. Thereby H_1 has both diagonal matrix elements such as $\langle\nu|H_1|\nu\rangle$ but also off-diagonal matrix elements $\langle\mu|H_1|\nu\rangle$. The diagonal matrix elements describe the fact that the Coulomb repulsion between two electrons in different orbitals depends on the spatial character of these orbitals whereas the off-diagonal matrix elements describe the scattering of two electrons from each other as shown in Figure 1.

In second quantization the Coulomb Hamiltonian H_1 takes the form

$$H_1 \;=\; \frac{1}{2} \sum_{i,j,k,l} V(\nu_i, \nu_j, \nu_k, \nu_l) \; c_{\nu_i}^\dagger c_{\nu_j}^\dagger c_{\nu_k} c_{\nu_l} \;,$$

$$V(\nu_1, \nu_2, \nu_3, \nu_4) \;=\; \int dx \int dx' \; \psi_{\nu_1}^*(x) \, \psi_{\nu_2}^*(x') \, V_c(x, x') \, \psi_{\nu_3}(x') \, \psi_{\nu_4}(x) \;,$$

$$V_c(x, x') \;=\; \frac{1}{|\boldsymbol{r} - \boldsymbol{r}'|} \;. \tag{2}$$

Here $x = (\boldsymbol{r}, \sigma)$ is the combined position and spin coordinate with $\int dx \cdots = \sum_\sigma \int d\boldsymbol{r} \ldots$ and V_c is the Coulomb interaction between electrons. Note the factor of $1/2$ in front of H_1 and the correspondence of indices and integration variables $\nu_3 \leftrightarrow x'$ and $\nu_4 \leftrightarrow x$ in the Coulomb matrix element, see textbooks of many-particle physics such as Fetter-Walecka [4].

2.2   The Coulomb matrix elements

Our single-particle basis consists of atomic spin-orbitals so if we switch to polar coordinates (r, ϑ, φ) for $\boldsymbol{r}$ the wave functions in (2) are

$$\psi_{\nu_i}(x) \;=\; R_{n_i, l_i}(r) \, Y_{l_i, m_i}(\vartheta, \varphi) \, \delta_{\sigma, \sigma_i}. \tag{3}$$

The radial wave functions R_{n_i, l_i} are assumed to be real, as is the case for the true radial wave function of bound states in a central potential. Apart from that we do not really specify them. In fact, it would be rather difficult to give a rigorous prescription for their determination. It will turn out, however, that these radial wave functions enter the Coulomb matrix elements only via a discrete and rather limited set of real numbers which are often obtained by a fit to experiment. In addition to (3), we use the familiar multipole expansion of the Coulomb interaction

$$\frac{1}{|\boldsymbol{r} - \boldsymbol{r}'|} \;=\; \sum_{k=0}^{\infty} \sum_{m=-k}^{k} Y_{k,m}^*(\vartheta', \varphi') \, \frac{4\pi}{2k+1} \, \frac{r_<^k}{r_>^{k+1}} \, Y_{k,m}(\vartheta, \varphi) \,. \tag{4}$$

We now insert (3) and (4) into (2). We recall that $\int dx \cdots = \sum_\sigma \int d\boldsymbol{r} \ldots$ and first carry out the sum over spin variables which gives a factor of $\delta_{\sigma_1, \sigma_4} \, \delta_{\sigma_2, \sigma_3}$. Next we pick one term with given k and m from the multipole expansion (4) and proceed to the integration over the spatial variables (r, ϑ, φ) and $(r', \vartheta', \varphi')$. Let us first consider the angular variables (ϑ, φ). Obviously these always come as arguments of spherical harmonics and there is one from $\psi_{\nu_1}^*(x)$, one from the multipole expansion (4), and one from $\psi_{\nu_4}(x)$. We thus obtain a factor of

$$\int_0^{2\pi} d\varphi \int_{-1}^{1} d\cos(\vartheta) \, Y_{l_1, m_1}^*(\vartheta, \varphi) \, Y_{k,m}(\vartheta, \varphi) \, Y_{l_4, m_4}(\vartheta, \varphi) \,. \tag{5}$$

Such a dimensionless integral over three spherical harmonics is called a Gaunt coefficient and can be shown to be proportional to a Clebsch-Gordan coefficient [5, 6]. This property is an immediate consequence of the Wigner-Eckart theorem.

Another interesting property can be seen if we recall the φ-dependence of the spherical harmonics: $Y_{l,m}(\vartheta, \varphi) = P_{l,m}(\vartheta) e^{im\varphi}$. It follows that the Gaunt coefficient (5) is different from zero only if $m_1 = m_4 + m$. Moreover, since the ϑ-dependent factors $P_{l,m}(\vartheta)$ are real [5,6] all nonvanishing Gaunt coefficients are real as well. In the same way the integration over (ϑ', φ') gives

$$\int_0^{2\pi} d\varphi' \int_{-1}^1 dcos(\vartheta') \, Y_{l_2,m_2}^*(\vartheta', \varphi') \, Y_{k,m}^*(\vartheta', \varphi') \, Y_{l_3,m_3}(\vartheta', \varphi'), \tag{6}$$

which by analogous reasoning is different from zero only if $m_2 + m = m_3$. Since both (5) *and* (6) must be different from zero for the *same* m in order to obtain a nonvanishing contribution, we must have $m_1 + m_2 = m_3 + m_4$. This is simply the condition that L^z be conserved in the Coulomb scattering of the two electrons.

It remains to do the integral over the two radial variables r and r'. These two integrations cannot be disentangled so we find a factor of

$$R^k(n_1 l_1, n_2 l_2, n_3 l_3, n_4 l_4) = \int_0^\infty dr \, r^2 \int_0^\infty dr' \, r'^2 \, R_{n_1 l_1}(r) \, R_{n_2 l_2}(r') \, \frac{r_<^k}{r_>^{k+1}} \, R_{n_3 l_3}(r') \, R_{n_4 l_4}(r) \,. \tag{7}$$

These integrals, which have the dimension of energy, are labeled by the multipole index k, and the number of relevant multipole orders is severely limited by the properties of the Gaunt coefficients: First, since the latter are proportional to Clebsch-Gordan coefficients the three l-values appearing in them have to obey the so-called *triangular condition* [3] whence $k \leq \min(|l_1 + l_4|, |l_2 + l_3|)$. For a d-shell where $l_i = 2$ it follows that $k \leq 4$. Second, the parity of the spherical harmonic Y_{lm} is $(-1)^l$, i.e. even for the case $l_i = 2$. For integrals such as (5) or (6) to be different from zero the spherical harmonic $Y_{k,m}$ from the multipole expansion must have even parity, too, so that for Coulomb scattering within a d-shell only R^0, R^2 and R^4 are relevant. This shows that the sloppy definition of the wave function $R_{n_i,l_i}(r)$ is not a real problem because details of this wave function are irrelevant anyway. In a way, these three parameters may be viewed as a generalization of the Hubbard-U in that R^k is something like the 'the Hubbard-U for k-pole interaction'.

We introduce the following notation for the nonvanishing Gaunt coefficients

$$c^k(lm; l'm') = \sqrt{\frac{4\pi}{2k+1}} \int_0^{2\pi} d\varphi \int_{-1}^1 d\cos(\vartheta) \, Y_{lm}^*(\vartheta, \varphi) \, Y_{k,m-m'}(\vartheta, \varphi) \, Y_{l',m'}(\vartheta, \varphi) \,. \tag{8}$$

These coefficients are tabulated in Appendix 20a of the textbook by Slater [5] or Table 4.4 of the textbook by Griffith [6], and also in the Appendix of this chapter. Using this notation and the fact that the Gaunt coefficients are real we can finally write the Coulomb matrix element as

$$V(\nu_1, \nu_2, \nu_3, \nu_4) = \delta_{\sigma_1,\sigma_4} \, \delta_{\sigma_2,\sigma_3} \, \delta_{m_1+m_2,m_3+m_4} \tag{9}$$

$$\times \sum_{k=0}^\infty c^k(l_1 m_1; l_4 m_4) \, c^k(l_3 m_3; l_2 m_2) \, R^k(n_1 l_1, n_2 l_2, n_3 l_3, n_4 l_4) \,.$$

$$459 = 0\ 1\ 1\ 1\ 0\ 0\ 1\ 0\ 1\ 1$$
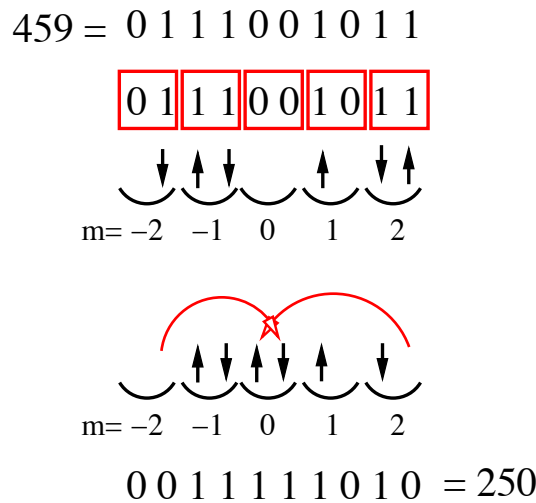

$$0\ 0\ 1\ 1\ 1\ 1\ 1\ 0\ 1\ 0\ = 250$$

Fig. 2: *The coding of basis states by integers and a scattering process.*

2.3 Solution of the Coulomb problem by exact diagonalization

We now describe how the problem of the partly filled $3d$-shell can be solved numerically, using the method of exact diagonalization. The basis states (1) correspond to all possible ways of distributing n electrons over the 10 spin-orbitals of the $3d$-shell (two spin directions for each $m \in \{-2, -1 \ldots 2\}$). As illustrated in Figure 2 we can code each of these basis states by an integer $0 \leq i \leq 2^{10}$. If we really use all of these integers we are actually treating all states with $0 \leq n \leq 10$ simultaneously but this will be convenient for later generalizations. Next, for a given initial state $|\nu_1, \nu_2, \ldots \nu_n\rangle$ we can let the computer search for all possible transitions of the type shown in Figure 1 and compute the corresponding matrix elements from (9) using, say, the $c^k(lm; l'm')$ copied from Slater's textbook and some given R^0, R^2 and R^4. Let us consider the following matrix element

$$\langle 0|c_{\mu_n} \ldots c_{\mu_1} V(\lambda_1, \lambda_2, \lambda_3, \lambda_4) c^\dagger_{\lambda_1} c^\dagger_{\lambda_2} c_{\lambda_3} c_{\lambda_4} c^\dagger_{\nu_1} c^\dagger_{\nu_2} \ldots c^\dagger_{\mu_n}|0\rangle .$$

For this to be nonzero, the operators $c^\dagger_{\lambda_3}$ and $c^\dagger_{\lambda_4}$ must be amongst the $c^\dagger_{\nu_i}$, otherwise the annihilation operators in the Hamiltonian could be commuted to the right where they annihilate $|0\rangle$. In order for these pairs of operators to cancel each other, c_{λ_4} must first be commuted to the position right in front of $c^\dagger_{\lambda_4}$. If this takes n_4 interchanges of Fermion operators we get a Fermi sign of $(-1)^{n_4}$. Bringing next c_{λ_3} right in front of $c^\dagger_{\lambda_3}$ by n_3 interchanges of Fermion operators gives a sign of $(-1)^{n_3}$. Analogously, the creation operators $c^\dagger_{\lambda_1}$ and $c^\dagger_{\lambda_2}$ have to be commuted to the left to stand to the immediate right of their 'partner annihilation operators' so as to cancel them. If this requires an additional number of Fermion interchanges n_2 for $c^\dagger_{\lambda_2}$ and n_1 for $c^\dagger_{\lambda_1}$ there is an additional Fermi sign of $(-1)^{n_1+n_2}$. The total matrix element then is $(-1)^{n_1+n_2+n_3+n_4} V(\lambda_1, \lambda_2, \lambda_3, \lambda_4)$. The correct Fermi sign is crucial for obtaining correct results and must be evaluated by keeping track of all necessary interchanges of Fermion operators. This is perhaps the trickiest part in implementing the generation of the Hamilton matrix or any other operator in a computer program.

E	S	L	n	Term	E	S	L	n	Term
0.0000	1	3	21	^3F	0.0000	3/2	3	28	^4F
1.8420	0	2	5	^1D	1.8000	3/2	1	12	^4P
1.9200	1	1	9	^3P	2.1540	1/2	4	18	^2G
2.7380	0	4	9	^1G	2.7540	1/2	5	22	^2H
13.2440	0	0	1	^1S	2.7540	1/2	1	8	^2P
					3.0545	1/2	2	10	^2D
					4.5540	1/2	3	14	^2F
					9.9774	1/2	2	10	^2D

Table 2: *Energies of the d^8 multiplets calculated with $R^2 = 10.479$ eV, $R^4 = 7.5726$ eV (Left), and energies of the d^7 multiplets calculated with $R^2 = 9.7860$ eV, $R^4 = 7.0308$ eV (Right).*

Once the matrix has been set up it can be diagonalized numerically. Table 2 gives the resulting multiplet energies for d^8 and d^7, the values of L and S for each multiplet and the degeneracy n. The values of the R^k parameters have been calculated by using Hartree-Fock wave functions $R_{3,2}$ for Ni^{2+} and Co^{2+} in (7). The energy of the lowest multiplet is taken as the zero of energy and it turns out that all *energy differences* depend only on R^2 and R^4. Note the increasing complexity of the level schemes with increasing number of holes in the d-shell. Comparing the energies of the multiplets for d^8 with the experimental values in Table 1 one can see good agreement with deviations of order 0.1 eV. The only exception is ^1S. This is hardly a surprise because here the theoretical energy is 13 eV which is comparable to the difference in energy between the $3d$ and the $4s$-shell in Ni (which is ≈ 10 eV). It follows that the basic assumption of the calculation, namely that the separation between atomic shells is large compared to the multiplet energies, is not fulfilled for this particular multiplet. To treat ^1S more quantitatively it would likely be necessary to include basis states with configurations like $3d^7\,4s^1$, or, put another way, to consider the screening of the Coulomb interaction by particle-hole excitations from the $3d$- into the $4s$-shell. Finally, the Table shows that the ground states indeed comply with the first two of Hund's rules: They have maximum spin and maximum orbital angular momentum for this spin. It can be shown that this is indeed always the case as long as one uses Coulomb and exchange integrals with the correct, i.e. positive, sign [5,6].

2.4   Diagonal matrix elements

The expression (9) is exact but looks somewhat complicated so let us try to elucidate its physical content and thereby also make contact with various approximate ways to describe the Coulomb interaction which can be found in the literature. We first consider those matrix elements where either $\nu_4 = \nu_1$ and $\nu_3 = \nu_2$ (case 1) or $\nu_3 = \nu_1$ and $\nu_4 = \nu_2$ (case 2). In both cases the four Fermion operators in the corresponding terms of H_1 can be permuted to give the product of number operators $n_{\nu_1} n_{\nu_2}$ (with $n_\nu = c_\nu^\dagger c_\nu$) whereby in case 2 an odd number of interchanges of Fermion operators is necessary so that an additional factor of (-1) appears. Whereas for case 1 the product $\delta_{\sigma_1,\sigma_4}\,\delta_{\sigma_2,\sigma_3}$ in (9) always is 1, it vanishes for case 2 unless $\sigma_1 = \sigma_2$. The Pauli

principle requires that $\nu_1 \neq \nu_2$ (otherwise one has the product $c^\dagger_{\nu_1} c^\dagger_{\nu_1} = 0$) so that for case 1 the two orbitals may have the same orbital quantum numbers n, l, m but then must differ in their spin, whereas in case 2 the spins have to be equal so that the orbital quantum numbers definitely must be different. Using (9) the respective matrix elements are

$$
\begin{aligned}
V(\nu_1, \nu_2, \nu_2, \nu_1) &= \sum_{k=0}^{\infty} c^k(l_1 m_1; l_1, m_1)\, c^k(l_2 m_2; l_2, m_2)\, R^k(n_1 l_1, n_2 l_2, n_2 l_2, n_1 l_1), \\
V(\nu_1, \nu_2, \nu_1, \nu_2) &= \delta_{\sigma_1 \sigma_2} \sum_{k=0}^{\infty} c^k(l_1 m_1; l_2, m_2)\, c^k(l_1 m_1; l_2, m_2)\, R^k(n_1 l_1, n_2 l_2, n_1 l_1, n_2 l_2).
\end{aligned}
$$
(10)

It is customary to introduce the following abbreviations

$$
\begin{aligned}
a^k(lm; l'm') &= c^k(lm; lm)\ \ c^k(l'm'; l'm') \\
b^k(lm; l'm') &= c^k(lm; l'm')\, c^k(lm; l'm') \\
F^k(nl; n'l') &= R^k(nl, n'l', n'l', nl) \\
G^k(nl; n'l') &= R^k(nl, n'l', nl, n'l')
\end{aligned}
$$

The F^k and G^k are called Slater-Condon parameters. The a^k and b^k are listed in Appendix 20a of Slater's textbook [5] and also the Appendix of the this chapter.

We now want to bring these diagonal matrix elements to a more familiar form and thereby specialize to a partly filled $3d$-shell. In this case all $n_i = 3$ and $l_i = 2$ so that for each k there is only one F^k and one G^k and, in fact, $G^k = F^k$. For brevity we omit the n and l quantum numbers in the rest of the paragraph so that, e.g., the electron operators become $c^\dagger_{m,\sigma}$ with m the z-component of $\boldsymbol{L}$. The sum of all diagonal matrix elements then becomes

$$
H_{1,diag} = \sum_{m} U_{m,m}\, n_{m,\uparrow} n_{m,\downarrow} + \frac{1}{2} \sum_{m \neq m'} \left(U_{m,m'} \sum_{\sigma,\sigma'} n_{m,\sigma} n_{m',\sigma'} - J_{m,m'} \sum_{\sigma} n_{m,\sigma} n_{m',\sigma} \right),
$$

$$
U_{m,m'} = \sum_{k \in \{0,2,4\}} a^k(m, m')\, F^k, \qquad J_{m,m'} = \sum_{k \in \{0,2,4\}} b^k(m, m')\, F^k.
$$

The first term on the right-hand side originates from case 1 with $m_1 = m_2$ and the factor of $1/2$ in front of this term is cancelled because there are two identical terms of this type with either $\nu_1 = (m, \uparrow)$ and $\nu_2 = (m, \downarrow)$ or $\nu_1 = (m, \downarrow)$ and $\nu_2 = (m, \uparrow)$. Defining $n_m = n_{m,\uparrow} + n_{m,\downarrow}$ and $S_m^z = (n_{m,\uparrow} - n_{m,\downarrow})/2$ we have

$$
\sum_{\sigma,\sigma'} n_{m,\sigma}\, n_{m',\sigma'} = n_m\, n_{m'} \qquad\qquad \sum_{\sigma} n_{m,\sigma}\, n_{m',\sigma} = 2 \left(S_m^z S_{m'}^z + \frac{n_m n_{m'}}{4} \right),
$$

so that

$$
H_{1,diag} = \sum_{m} U_{m,m}\, n_{m,\uparrow}\, n_{m,\downarrow} + \frac{1}{2} \sum_{m \neq m'} \left((U_{m,m'} - \frac{1}{2} J_{m,m'})\, n_m n_{m'} - 2 J_{m,m'}\, S_m^z S_{m'}^z \right).
$$

This is the sum of a Hubbard-like density interaction $\propto U_{m,m'}$ and an Ising-like spin interaction $\propto J_{m,m'}$. The interaction parameters thereby depend on the orbitals and can be expressed in terms of the Slater Condon parameters F^k and the products of Gaunt coefficients a^k and b^k. It is obvious that $J_{m,m'} > 0$ so that the Ising-like interaction describes ferromagnetic coupling — as one would expect on the basis of the first Hund's rule. A truncated Coulomb Hamiltonian like $H_{1,diag}$ is used in some LDA+U schemes [7] and also in many Dynamical Mean-Field calculations for $3d$ transition-metal compounds [8].

To complete the Hund's rule term we consider in addition those terms in H_1 where $\nu_1 = (m, \sigma)$, $\nu_2 = (m', \bar{\sigma})$, $\nu_3 = (m, \bar{\sigma})$ and $\nu_4 = (m', \sigma)$. In these terms the product $\delta_{\sigma_1,\sigma_4}\,\delta_{\sigma_2,\sigma_3}$ is nonvanishing as well and for both values of σ the matrix element (2) is

$$\sum_{k \in \{0,2,4\}} c^k(m, m')\, c^k(m, m')\, F^k = \sum_{k \in \{0,2,4\}} b^k(m, m')\, F^k = J_{m,m'}$$

The Fermion operators are $c^\dagger_{m,\uparrow} c^\dagger_{m',\downarrow} c_{m,\downarrow} c_{m',\uparrow} + c^\dagger_{m,\downarrow} c^\dagger_{m',\uparrow} c_{m,\uparrow} c_{m',\downarrow} = -(S^+_m S^-_{m'} + S^-_m S^+_{m'})$, i.e., the transverse part of the Heisenberg exchange. Combining these terms with the Ising-like spin exchange term we obtain

$$H_{1,H} = \sum_m U_{m,m}\, n_{m,\uparrow}\, n_{m,\downarrow} + \frac{1}{2} \sum_{m \neq m'} \left((U_{m,m'} - \frac{1}{2}J_{m,m'})\, n_m n_{m'} - 2 J_{m,m'}\, \boldsymbol{S}_m \cdot \boldsymbol{S}_{m'} \right).$$

This is now the sum of a density interaction and a spin-rotation invariant ferromagnetic spin exchange. It has to be kept in mind that this Hamiltonian has been obtained by retaining only a relatively small subset of matrix elements in the original Coulomb Hamiltonian. A further simplification which is often used is to replace $U_{m,m'}$ and $J_{m,m'}$ by their averages over all corresponding pairs (m, m'). Using the a^k and b^k in the Appendix one readily obtains

$$U = \frac{1}{25} \sum_{m,m'} U_{m,m'} = F^0,$$

$$U - J = \frac{1}{20} \sum_{m \neq m'} (U_{m,m'} - J_{m,m'}) = F^0 - \frac{1}{14}(F^2 + F^4),$$

so that $J = (F^2 + F^4)/14$.

To conclude the discussion, we consider the diagonal matrix elements $\langle \nu | H_1 | \nu \rangle$ in the basis of n-electron states $|\nu\rangle$ defined in (1). Since ν_1 and ν_2 in (10) can be any two out of the n occupied orbitals in $|\nu\rangle$ the total diagonal matrix element of H_1 is obtained by summing over all $\frac{n(n-1)}{2}$ pairs (i, j) formed from the occupied orbitals

$$\langle \nu | H_1 | \nu \rangle = \sum_{i<j} \sum_k \left(a^k(l_i m_i, l_j, m_j)\, F^k(n_i l_i, n_j l_j) - \delta_{\sigma_i \sigma_j}\, b^k(l_i m_i, l_j, m_j)\, G^k(n_i l_i, n_j l_j) \right).$$

(11)

As will be seen in the next paragraph, this formula is sufficient for the analytical calculation of the multiplet energies.

2.5 Analytical calculation of multiplet energies by the diagonal sum-rule

The exact diagonalization procedure outlined in Sec. 2.3. can be used to obtain all eigenenergies and the corresponding eigenstates of the Coulomb problem. It is a flexible numerical method of solution into which crystalline electric field, hybridization with ligand orbitals, spin-orbit coupling, and Coulomb interaction with holes in core shells, which is important for the discussion of X-ray absorption spectra, can be incorporated easily. On the other hand, multiplet theory was invented during the 1920's to explain the spectra of free atoms or ions, and at that time computers were not available. It turns out, however, that despite the apparent complexity of the problem the energies of the multiplets can be obtained analytically and this will be described in the following.

The first ingredient is the so-called diagonal sum-rule. This is simply the well-known theorem that the sum of the eigenvalues of a Hermitian matrix H is equal to its trace $\text{Tr}(H) = \sum_i H_{ii}$. It follows immediately by noting that the trace of a matrix is invariant under basis transformations, i.e., $\text{Tr}(H) = \text{Tr}(UHU^{-1})$ for any unitary matrix U. By choosing U to be the matrix which transforms to the basis of eigenvectors of H the diagonal sum-rule follows immediately.

Next, one uses the fact that the Hamilton matrix is block-diagonal, with blocks defined by their values of L^z and S^z. The diagonal sum-rule then can be applied separately for each of these blocks. In addition, the dimension of the blocks decreases as L^z and S^z approach their maximum possible values so that the number of multiplets contained in a given block increases.

As an example for the procedure let us consider a p^2 configuration (by particle-hole symmetry this is equivalent to a p^4 configuration). We write the Fermion operators in the form $c_{l,m,\sigma}$, i.e., we suppress the principal quantum number n. Since we have 6 possible states for a single p-electron (three m-values and two spin directions per m-value) we have 15 states for two electrons. The triangular condition implicit in the Gaunt coefficients now restricts the multipole order k to be ≤ 2. Again, only even k contribute, so that we have two Slater-Condon parameters, F^0 and F^2 (and $F^k = G^k$). The following Table which is taken from Slater's textbook [5] gives the values of the coefficients $a^k(1, m; 1, m')$ and $b^k(1, m; 1, m')$: We first consider the sector with $S^z = 1$. The highest possible L^z is $L^z = 1$ which is realized only for a single state, $|1\rangle = c^\dagger_{1,0,\uparrow} c^\dagger_{1,1,\uparrow} |0\rangle$. We can conclude that one of the multiplets is ^3P and its energy is equal to

Table 3: *The coefficients a^k and b^k for two p-electrons.*

m	m'	a^0	$25a^2$	b^0	$25b^2$
± 1	± 1	1	1	1	1
± 1	0	1	-2	0	3
0	0	1	4	1	4
± 1	∓ 1	1	1	0	6

the diagonal matrix element of $|1\rangle$ which by (11) is

$$E(^3P) = \sum_{k \in \{0,2\}} \left(a^k(1,1;1,0) - b^k(1,1;1,0)\right) F^k = F^0 - \frac{5}{25} F^2.$$

We proceed to the sector $S^z = 0$. Here the highest possible L^z is $L^z = 2$ again obtained for only single state namely $c^\dagger_{1,1,\downarrow} c^\dagger_{1,1,\uparrow} |0\rangle$. We conclude that we also have ^1D with energy

$$E(^1D) = \sum_{k \in \{0,2\}} a^k(1,1;1,1) F^k = F^0 + \frac{1}{25} F^2.$$

The two multiplets that we found so far, ^1D and ^3P, comprise $5 + 9 = 14$ states – we thus have just one state missing, which can only be ^1S. To find its energy, we need to consider the sector $S^z = 0$ and $L^z = 0$. There are three states in this sector: $c^\dagger_{1,0,\downarrow} c^\dagger_{1,0,\uparrow} |0\rangle$, $c^\dagger_{1,-1,\uparrow} c^\dagger_{1,1,\downarrow} |0\rangle$ and $c^\dagger_{1,-1,\downarrow} c^\dagger_{1,1,\uparrow} |0\rangle$. Two out of the three eigenvalues of the 3×3 Hamiltonian in the basis spanned by these states must be $E(^3P)$ and $E(^1D)$, because these multiplets also have members with $S^z = 0$ and $L^z = 0$. To obtain $E(^1S)$ we accordingly compute the sum of the diagonal elements of the 3×3 matrix and set

$$E(^3P) + E(^1D) + E(^1S) = \sum_{k \in \{0,2\}} \left(a^k(1,0;1,0) + 2\,a^k(1,-1;1,1)\right) F^k$$

$$\rightarrow E(^1S) = F^0 + \frac{10}{25} F^2.$$

This example shows the way of approach for multiplet calculations using the diagonal sum-rule: one starts out with a state with maximum L^z or S^z for which there is usually only a single basis state. This basis state belongs to some multiplet whose energy simply equals the 'diagonal element' of the 1×1 Hamiltonian. Then one proceeds to lower S^z and/or L^z and obtains energies of additional multiplets by calculating the trace of the respective block of the Hamilton matrix and using the known energies of multiplets with higher L^z or S^z. It turns out that in this way the energies of *all* multiplets involving s, p, d or f electrons can be expressed in terms of the Slater-Condon parameters by analytical formulas. A rather complete list can be found for example in the Appendices 21a and 21b of the textbook by Slater [5].

One point which may be helpful when reading the literature is the following: for the special case of a partly filled d-shell many authors use the so-called Racah parameters A, B, and C instead of the 3 Slater-Condon parameters F^0, F^2, and F^4. The rule for conversion is simple:

$$A = F^0 - \frac{49}{441} F^4 \qquad\qquad B = \frac{1}{49} F^2 - \frac{5}{441} F^4 \qquad\qquad C = \frac{35}{441} F^4.$$

The Racah-parameters have been introduced because the analytical formulas for the energies of the multiplets of d^n as derived by the diagonal sum-rule look nicer when they are expressed in terms of them. For example Griffith [6] gives multiplet energies in terms of the Racah-parameters in his Table 4.6.

As stated above, multiplet theory was originally developed to discuss the spectra of atoms or

p^2	C	N^+	O^{2+}	Si	P^+	S^{2+}
	1.124	1.134	1.130	1.444	1.430	1.399
p^4	O	F^+		S	Cl^+	
	1.130	1.152		1.401	1.392	

Table 4: *The ratio (12) for various Atoms and Ions with p^2 and p^4 configurations outside a closed shell.*

ions in the gas phase. The question then arises, as to what are the values of the Slater-Condon parameters. Of course one might attempt to compute these parameters using, e.g., Hartree-Fock wave functions in the expression (7). It turns out, however, that very frequently the number of multiplets considerably exceeds the number of relevant Slater-Condon parameters. In the case of the p^2 configuration we had three multiplets, ^3P, ^1D, and ^1S, but only two Slater-Condon parameters F^0 and F^2. This would suggest to obtain the values of the Slater-Condon parameters by fit to the spectroscopic data and the textbook by Slater [5] contains a vast amount of experimental data which are analyzed in this way. For the p^2 configuration we restrict ourselves to a simple cross check. Using the above formulae and eliminating the F's we find:

$$r = \frac{E(^1S) - E(^1D)}{E(^1D) - E(^3P)} = \frac{3}{2}. \tag{12}$$

This relation should be obeyed by all ions with two p-electrons outside filled shells, e.g., the series C, N^{1+} and O^{2+} or two holes in a filled p-shell such as the series O and F^+. The energies of these multiplets have been measured with high precision and are available in databases [2] and Table 4 shows the resulting values of r. For the first-row elements the deviation is about 25%, for the second row only about 5%. We recall that multiplet theory corresponds to first order degenerate perturbation theory, where H_0 contains the orbital energies and H_1 the Coulomb interaction between electrons in one shell. It therefore will work the better the larger the separation between different atomic shells and this is indeed larger in the second row elements.

2.6 Spin-orbit coupling

As the last problem in this section on free atoms or ions we briefly discuss spin-orbit coupling. The corresponding Hamiltonian is

$$H_{SO} = \lambda_{SO} \sum_{i=1}^{n} \boldsymbol{l}_i \cdot \boldsymbol{S}_i = \lambda_{SO} \sum_{i=1}^{n} \left(l_i^z S_i^z + \frac{1}{2}(l_i^+ S_i^- + l_i^- S_i^+) \right).$$

where $\boldsymbol{l}_i$ ($\boldsymbol{S}_i$) are the operator of orbital (spin) angular momentum of the ith electron. The spin-orbit coupling constant λ_{SO} can be written as [3]

$$\lambda_{SO} = \frac{\hbar^2}{2m_e^2 c^2 r_{orb}} \left. \frac{dV_{at}}{dr} \right|_{r=r_{orb}}$$

where m_e is the electron mass, c the speed of light, V_{at} is the atomic potential acting on the electron, and r_{orb} the spatial extent of the radial wave function.

The first term on the right hand side can be translated into second quantized form easily:

$$H_{SO}^{\parallel} = \lambda_{SO} \sum_{m=-l}^{l} \frac{m}{2} \left(c_{l,m,\uparrow}^{\dagger} c_{l,m,\uparrow} - c_{l,m,\downarrow}^{\dagger} c_{l,m,\downarrow} \right). \tag{13}$$

As regards the transverse part, we note [3] that the only nonvanishing matrix elements of the orbital angular momentum raising/lowering operator are $\langle l, m\pm 1|l^{\pm}|l, m\rangle = \sqrt{(l \mp m)(l \pm m + 1)}$ whence

$$H_{SO}^{\perp} = \frac{\lambda_{SO}}{2} \sum_{m=-l}^{l-1} \sqrt{(l-m)(l+m+1)} \left(c_{l,m+1,\downarrow}^{\dagger} c_{l,m,\uparrow} + c_{l,m,\uparrow}^{\dagger} c_{l,m+1,\downarrow} \right). \tag{14}$$

Spin-orbit coupling can be implemented rather easily into the numerical procedure, the main difficulty again is keeping track of the Fermi sign. Due to the fact that neither L^z nor S^z are conserved anymore the corresponding reduction of the Hilbert space is no longer possible. In transition-metal compounds the spin-orbit coupling constant λ_{SO} for the $3d$-shell is rather small, of order $\lambda_{SO} \approx 0.05$ eV. Still, if the ground state of a given ion has a non-vanishing spin, spin-orbit coupling will determine how this spin orients itself in an ordered phase giving rise to a *magnetic anisotropy*. In the rare-earth elements spin-orbit coupling in the $4f$-shell is of comparable magnitude as the Coulomb repulsion. There, taking spin-orbit coupling into account is mandatory.

3 Effects of the environment in the crystal

So far we have considered a single ion in vacuum. Clearly, one might ask if the results obtained in this limit retain any relevance once the ion is embedded into a solid and this will be discussed in the following. One may expect, however, that the small spatial extent of the $3d$ radial wave function $R_{3,2}(r)$ suppresses any effect of the environment in a solid, so that in many cases the main effect of embedding the ion into a solid is the partial splitting of the multiplets of the free ion.

In many transition-metal compounds the $3d$ ions are surrounded by an approximately octahedral or tetrahedral 'cage' of nonmetal ions such as Oxygen, Sulphur, Arsenic. These nearest neighbor ions, which will be called 'ligands' in the following, have a two-fold effect: first, they produce a static electric field, the so-called *crystalline electric field* or CEF, and second there may be *charge transfer*, that means electrons from a filled ligand orbital may tunnel into a $3d$-orbital of the transition-metal ion and back due to the overlap of the respective wave functions.

3.1 Crystalline electric field

The electric field that acts on a given ion in a solid may to simplest approximation be obtained by representing the other ions in the solid as point charges. The electrostatic potential $V_{CEF}(\boldsymbol{r})$

produced by these point charges around the nucleus in question then in principle can be obtained by using the multipole expansion (4). This results in an expression of the type

$$V_{CEF}(\boldsymbol{r}) \;=\; \sum_{l=0}^{\infty} \sum_{m=-l}^{l} C_{l,m} \, r^l \, Y_{l,m}(\vartheta, \varphi)$$

where the coefficients $C_{l,m}$ depend on the geometry of the crystal. Matrix elements of $V_{CEF}(\boldsymbol{r})$ between atomic eigenfunctions of the type (3) can be calculated by applying similar procedures as in the computation of the Coulomb matrix elements (and in particular again involve Gaunt coefficients).

However, such calculations often do not give very accurate numbers. For example, there will always be some charge transfer between the ions in the solid so that it is difficult to decide which charge should be assigned to a given ion. Moreover, the calculation of matrix elements involves a radial integral over the wave function $R_{n,l}(r)$ which is not really well known. Therefore, we give a qualitative discussion based on symmetry.

Let α be some symmetry operation, i.e. a coordinate transformation represented by a unitary 3×3 matrix m_α, that leaves the environment of the ion in question invariant. In other words, the transition-metal ion itself must be transformed into itself whereas every other ion must be transformed into an ion of the same species. Then we define for any function of the coordinates $f(\boldsymbol{r})$ the operator $T_\alpha f(\boldsymbol{r}) = f(m_\alpha^{-1}\boldsymbol{r})$. Thus, if we want to know the value of $T_\alpha f(\boldsymbol{r})$ at some given point $\boldsymbol{r}$, we can look it up by evaluating the original function $f(\boldsymbol{r})$ at the point $\boldsymbol{r}' = m_\alpha^{-1}\boldsymbol{r}$ which is transformed into $\boldsymbol{r}$ by the operation α. In other words, if we imagine functions of $\boldsymbol{r}$ to be represented by color maps in real space, the map of $T_\alpha f(\boldsymbol{r})$ is that of $f(\boldsymbol{r})$ but subject to the transformation α. Since the charge density of the environment is invariant under the allowed symmetry operations, the same holds true for its electrostatic potential $V_{CEF}(\boldsymbol{r})$ so that $T_\alpha \, V_{CEF}(\boldsymbol{r}) = V_{CEF}(\boldsymbol{r})$. It follows that the Hamiltonian $\tilde{H} = H_{ion} + V_{CEF}(\boldsymbol{r})$ (where H_{ion} is the sum of the nuclear potential of the transition-metal ion, the kinetic energy of the electrons and their Coulomb interaction) commutes with T_α. It is then straightforward to show that if $\psi(\boldsymbol{r})$ is an eigenstate of $\tilde{H}$ with energy E, $\tilde{H}\,\psi(\boldsymbol{r}) = E\,\psi(\boldsymbol{r})$, the transformed function $T_\alpha\,\psi(\boldsymbol{r})$ is an eigenstate to the same energy:

$$[\tilde{H}, T_\alpha]\psi(\boldsymbol{r}) = 0 \quad \Rightarrow \quad \tilde{H}\,(T_\alpha\psi(\boldsymbol{r})) = T_\alpha E\,\psi(\boldsymbol{r}) = E\,(T_\alpha\psi(\boldsymbol{r})).$$

We can thus investigate to what degree the degeneracy of the five $3d$-orbitals is lifted in a given environment by systematically studying which (combinations of) $3d$-orbitals are transformed into each other by the symmetry operations which leave the environment invariant. For the general case this can be done by invoking the very elegant mathematical formalism of group theory [6, 9]. On the other hand, for an environment with cubic symmetry a simple shortcut is possible. Namely all 48 cubic symmetry operations can be expressed as the product of one of the 6 permutations of the 3 coordinate axis and one of the $2^3 = 8$ transformations which change the signs of an arbitrary subset of the 3 coordinates. Moreover the d-like spherical harmonics $Y_{2,m}$ can be expressed as linear combinations of products of two of the three components of the

unit vector $r/|r|$, such as xy/r^2 or z^2/r^2. For example

$$Y_{2,2}(\vartheta,\varphi) \;=\; \frac{1}{\sqrt{4\pi}}\;\sqrt{\frac{15}{8}}\;\sin^2\vartheta\;e^{\,2i\varphi} = \frac{1}{\sqrt{4\pi}}\;\sqrt{\frac{15}{8}}\;\left(\frac{x^2-y^2}{r^2}+2i\;\frac{xy}{r^2}\right).$$

It is then obvious that under cubic operations mixed products such as xy/r^2 will be transformed into mixed products, whereas squares such as z^2/r^2 will be transformed into squares. Thus, if we form linear combinations of the spherical harmonics which consist exclusively of either mixed products or squares, we know that these two groups of linear combinations will remain degenerate in the cubic environment. In fact, the mixed products are precisely the three t_{2g}-orbitals

$$\begin{aligned}
d_{xy} &= \frac{i}{\sqrt{2}}\;(Y_{2,-2}-Y_{2,2}) = \sqrt{\frac{15}{4\pi}}\;\frac{xy}{r^2}\,,\\[4pt]
d_{yz} &= \frac{i}{\sqrt{2}}\;(Y_{2,-1}+Y_{2,1}) = \sqrt{\frac{15}{4\pi}}\;\frac{yz}{r^2}\,,\\[4pt]
d_{xz} &= \frac{1}{\sqrt{2}}\;(Y_{2,-1}-Y_{2,1}) = \sqrt{\frac{15}{4\pi}}\;\frac{xz}{r^2}\,,
\end{aligned} \tag{15}$$

whereas from the squares the two e_g-orbitals can be formed:

$$\begin{aligned}
d_{x^2-y^2} &= \frac{1}{\sqrt{2}}\;(Y_{2,-2}+Y_{2,2}) = \sqrt{\frac{15}{16\pi}}\;\frac{x^2-y^2}{r^2}\,,\\[4pt]
d_{3z^2-r^2} &= Y_{2,0} = \sqrt{\frac{5}{16\pi}}\;\frac{3z^2-r^2}{r^2}\,.
\end{aligned} \tag{16}$$

There are only two e_g-orbitals because one special combination of the squares, namely r^2, is transformed into itself under all symmetry operations. In a cubic environment, the 5-fold degenerate d-level therefore *always* splits into the 3-fold degenerate t_{2g}-level and the 2-fold degenerate e_g-level. The energy difference between the two e_g- and the three t_{2g}-orbitals is called $10Dq$ for historical reasons. The above discussion can be summarized in the operator for the electrostatic potential of an environment with cubic symmetry:

$$H_{CEF} = C - 4Dq \sum_{\alpha\in t_{2g},\sigma} c^\dagger_{\alpha,\sigma}c_{\alpha,\sigma} + 6Dq \sum_{\alpha\in e_g,\sigma} c^\dagger_{\alpha,\sigma}c_{\alpha,\sigma}\,.$$

The constant C, which gives the center of gravity of the energies of the five orbitals, is largely irrelevant. By expressing the e_g and t_{2g} harmonics d_α in terms of the original $Y_{l=2,m}$ via (15) and (16) we can thus represent H_{CEF} as a quadratic form in the original $c^\dagger_\nu$-operators. This quadratic form involves the splitting $10Dq$ as a parameter, so that this way of dealing with the crystalline electric field is very similar in spirit to our treatment of the Coulomb interaction in that details of the radial wave functions $R_{n,l}(r)$ are absorbed into a parameter which may be adjusted to experiment. Alternatively, the numerical value of $10Dq$ for a given solid may also be obtained from a fit to an LDA band structure. By adding H_{CEF} to the Hamiltonian for the intra-atomic Coulomb interaction we can now discuss the splitting of the original multiplets of the free ion
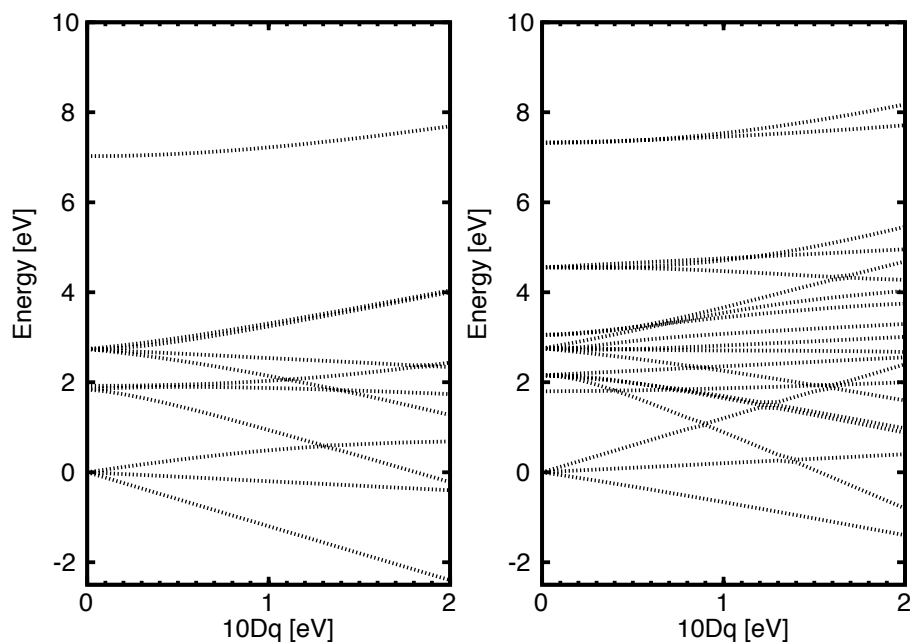
Fig. 3: *Examples for Tanabe-Sugano diagrams: the splitting of multiplets of* d^8 *(left) and* d^7 *(right) for increasing* $10Dq$. *The Slater-Condon parameters have the values given in Table 3.*

under the influence of the electrostatic potential of the environment. The following should be noted: the above discussion refers to the wave function of a *single electron*. The multiplets, however, are collective eigenstates of all n electrons in an atomic shell which are created by the Coulomb interaction between electrons. The question of how these collective states split in a cubic environment is not at all easy to answer. One way would be exact diagonalization including the term H_{CEF}. Plots of the energies of the resulting crystal-field multiplets versus $10Dq$ are called Tanabe-Sugano diagrams [10]. An example is shown in Figure 3.1 which shows the eigenenergies of the d^8 and d^7 configuration with Coulomb interaction and cubic CEF as $10Dq$ is increasing. One realizes that the highly degenerate multiplets of the free ion are split into several levels of lower degeneracy by the CEF, which is to be expected for a perturbation that lowers the symmetry. Note that the components into which a given multiplet splits up all have the same spin as the multiplet itself. This is because the spin of an electron does not feel an electrostatic potential — or, more precisely, because the operator of total spin commutes with any operator which acts only on the real-space coordinates r_i of the electrons.

An interesting example for the application of the Tanabe-Sugano diagrams are transition-metal ions in aqueous solution. In fact, the preference of transition-metal ions for an environment with cubic symmetry is so strong that such immersed ions often surround themselves with an octahedron of water molecules. Thereby the dipole moments of these six molecules all point away from the ion and thus create an electric field which cubic symmetry which again gives rise to the e_g-t_{2g} splitting. Optical transitions between the CEF-split multiplets, which are possible only due to slight distortions of the octahedron or the generation/annihilation of vibrational quanta during the transition, correspond to frequencies in the visible range and result in the charac-

teristic colors of such solutions. The Tanabe-Sugano diagrams have proved to be a powerful tool to understand the absorption spectra of such solutions [6]. By matching the energies of the observed transitions to energy differences in the Tanabe-Sugano diagrams one can extract estimates for the Slater-Condon parameters and for $10Dq$. The values of the Slater-Condon parameters are somewhat smaller than those for ions in vacuum due to dielectric screening in the solution. An independent estimate for $10Dq$ can also be extracted from measured heats of hydration (this is because both $10Dq$ and the electrostatic energy of the system 'ion plus octahedron' depend on the distance between the transition-metal ion and the water molecules) and compared to the estimate from the absorption spectrum whereby reasonable agreement is usually obtained [9].

3.2   Charge transfer

We proceed to a discussion of charge transfer. This means that electrons can tunnel from ligand orbitals into $3d$-orbitals, so that the number of electrons in the d-shell fluctuates. To deal with this we need to enlarge our set of Fermion operators $c_\nu^\dagger/c_\nu$ by operators $l_\mu^\dagger/l_\mu$ which create/annihilate electrons in orbitals centered on ligands. The compound index μ for the ligand operators also must include the index i of the ligand: $\mu = (i, n, l, m, \sigma)$. The Hamiltonian describing the charge transfer then would read

$$H_{kin} = \sum_{i,j} \left(t_{\nu_i,\mu_j}\, c_{\nu_i}^\dagger\, l_{\mu_j} + H.c. \right) + \sum_j \epsilon_{\mu_j}\, l_{\mu_j}^\dagger\, l_{\mu_j} + \sum_i \epsilon_{\nu_i}\, c_{\nu_i}^\dagger\, c_{\nu_i}\,. \tag{17}$$

The *hybridization integrals* t_{ν_i,μ_j,ν_j} may be expressed in terms of relatively few parameters by using the famous *Slater-Koster tables*, see the lecture by M. Foulkes [11] at this school. For example, if only the p-orbitals of the ligands are taken into account there are just two relevant parameters, $V_{pd\sigma}$ and $V_{pd\pi}$. Estimates for these may be obtained from fits to LDA band structures. If electrons are allowed to tunnel between d-shell and ligand orbitals the orbital energies ϵ_{μ_j} become relevant as well. Estimating the d-shell orbital energies from LDA calculations is tricky due to the *double counting problem*: the energies of the d-orbitals extracted from band structure calculations include the Hartree-potential, which is also included in the diagonal matrix elements of the Coulomb interaction and thus must be subtracted in some way.

We now specialize to the case where the ligands are oxygen ions which form an ideal octahedron with the transition-metal ion in the center of gravity of the octahedron. Retaining only the three oxygen $2p$-orbitals per ligand the total number of orbitals in this cluster would be $5 + 6 \cdot 3 = 23$ per spin direction which is far too big to be treated by exact diagonalization. However, the number of ligand orbitals can be reduced drastically if we note that for each of the real-valued transition-metal $3d$-orbitals $Y_\alpha(\vartheta, \varphi)$ there is precisely one linear combination of O $2p$-orbitals on the ligands, L_α, which hybridizes with it. The first term on the right-hand side of (17) then simplifies to

$$H_{hyb} = 2\,V_{pd\pi} \sum_{\alpha \in t_{2g}} \sum_\sigma \left(c_{\alpha,\sigma}^\dagger\, l_{\alpha\sigma} + H.c. \right) + \sqrt{3}\,V_{pd\sigma} \sum_{\alpha \in e_g} \sum_\sigma \left(c_{\alpha,\sigma}^\dagger\, l_{\alpha\sigma} + H.c. \right).$$

By inserting the unitary transformation (15) and (16) to transform to the original complex spherical harmonics this is easily included into the formalism. In the exact diagonalization program this means that the number of orbitals has to be doubled, because we have the five linear combinations L_α, each of which can accommodate an electron of either spin direction. This leads to a quite drastic increase in the dimension of the Hilbert space but using, e.g., the Lanczos algorithm, see e.g. Ref. [12], the problem still is tractable.

In constructing model-Hamiltonian-like descriptions of transition-metal compounds for which clusters containing several unit cells can be studied by exact diagonalization or quantum Monte Carlo, one can often find (approximate) analytical solutions by taking the limit of large $10Dq$. Then, one may restrict the basis to states where the numbers of electrons in the t_{2g} and e_g-orbitals are fixed. For example, for Ni^{2+} (i.e. d^8) in cubic symmetry one may assume that the six t_{2g}-orbitals always are completely filled. Then, one need to consider only the two electrons in the partially filled e_g level, resulting in a significant reduction of the number of possible basis states. Similarly, for early transition-metal compounds one often assumes that the e_g-orbitals are so high in energy that only the t_{2g}-orbitals need to be taken into account. Since it is the Coulomb interaction which reshuffles electrons between the five d-orbitals, the errors in these simplified models obviously are of order $F^2/10Dq$ or $F^4/10Dq$. In making such approximations it is advantageous to transform the Coulomb matrix elements (9) to real spherical harmonics. This is trivial, although tedious, because they are related by the unitary transformation (15), (16).

4 Cluster calculation of photoemission and X-ray absorption spectra

In the preceding section we have discussed the general formalism for exact diagonalization of a cluster consisting of a transition-metal ion and its nearest neighbor ions (ligands). Thereby the following terms were included into the Hamiltonian: the Coulomb repulsion between the electrons in the $3d$-shell, the electrostatic field produced by the other ions in the crystal, charge transfer between the ligands and the transition metal $3d$-orbitals and (possibly) the spin-orbit coupling in the $3d$-shell. By diagonalizing the resulting Hamilton matrix we can obtain the eigenfunctions $|\Psi_\nu\rangle$ and their energies E_ν and these can be used to simulate various experiments on transition-metal compounds such as electron spectroscopy, optical spectroscopy, electron spin resonance or inelastic neutron scattering. It has turned out that these simulations are in fact spectacularly successful. In many cases calculated spectra can be overlaid with experimental ones and agree peak by peak. Nowadays complete packages for such cluster simulations are available, and these are used routinely for the interpretation of, e.g., electron spectroscopy [13]. This shows in particular that the multiplets of the free ion, suitably modified by the effects of crystalline electric field and charge transfer, persist in the solid and thus are essential for a correct description of transition-metal compounds. In the following we want to explain this in more detail and consider photoelectron spectroscopy and X-ray absorption. In this lecture only a very cursory introduction can be given, there are however several excellent reviews on the

application of multiplet theory to the simulation of such experiments [14–16].

In a valence-band photoemission experiment electromagnetic radiation impinges on the sample which then emits electrons. This is nothing but the well-known photoeffect. Valence band photoemission means that the photoelectrons are ejected from states near the Fermi level so that to simplest approximation an ion in the solid undergoes the transition $d^n \rightarrow d^{n-1}$ (note that this ignores charge transfer, which in fact is quite essential!). What is measured is the current I of photoelectrons as a function of their kinetic energy E_{kin} and possibly the polar angles (ϑ, φ) relative to the crystallographic axes of the sample. Frequently one measures the angle-integrated spectrum, obtained by averaging over (ϑ, φ) or rather by measuring a polycrystalline sample. A further parameter, which strongly influences the shape of the spectrum $I(E_{kin})$, is the energy $h\nu$ of the incident photons. At sufficiently high $h\nu$ the photoionization cross-section for the transition-metal $3d$-orbitals is significantly larger than for the other orbitals in the solid so that the photoelectrons in fact are emitted almost exclusively from the $3d$-orbitals. This is often called XPS for X-ray photoemission spectroscopy.

The theory of the photoemission process is complicated [17, 18] but with a number of simplifying assumptions one can show that the photocurrent $I(E_{kin})$ measured in angle-integrated photoemission at high photon energy is proportional to the so-called single-particle spectral function

$$
\begin{aligned}
A(\omega) &= -\frac{1}{\pi Z} \Im \sum_{m=-2}^{2} \sum_{\mu} e^{-\beta E_\mu} \left\langle \Psi_\mu \left| c_{3,2,m,\sigma}^\dagger \frac{1}{\omega + (H - E_\mu) + i0^+} c_{3,2,m,\sigma} \right| \Psi_\mu \right\rangle \\
&= \frac{1}{Z} \sum_{m=-2}^{2} \sum_{\mu,\nu} e^{-\beta E_\mu} \left| \langle \Psi_\nu | c_{3,2,m,\sigma} | \Psi_\mu \rangle \right|^2 \delta(\omega + (E_\nu - E_\mu)).
\end{aligned} \tag{18}
$$

Here H is the Hamiltonian describing the solid, $|\Psi_\mu\rangle$ and E_μ denote the eigenstates and eigenenergies of H with a fixed electron number N_e. Moreover, $\beta = (k_B T)^{-1}$ with k_B the Boltzmann constant and T the temperature, and $Z = \sum_\mu \exp(-\beta E_\mu)$. The operator $c_{3,2,m,\sigma}$ removes an electron from a $3d$-orbital. In the thermodynamical limit the results will not depend on the position of the ion in the sample and accordingly we have suppressed the site index on $c_{3,2,m,\sigma}$. After removal of the electron the sample then remains in an eigenstate $|\Psi_\nu\rangle$ with $N_e - 1$ electrons and energy E_ν. The relation between E_{kin} and ω follows from energy conservation:

$$
h\nu + E_\mu = E_{kin} + \Phi + E_\nu
$$

The left- and right-hand sides of this equation are the energies of the system before (solid + photon) and after (solid + photoelectron) the photoemission process. Thereby Φ is the so-called work function, i.e., the energy needed to transverse the potential barrier at the surface of the solid (this needs to be introduced because the measured kinetic energy E_{kin} is the one *in vacuo*). It follows from the δ-function in the second line of (18) that we have to put $I(E_{kin}) \propto A(E_{kin} + \Phi - h\nu)$.

We now make an approximation, introduced by Fujimori and Minami [19], and evaluate $A(\omega)$ by replacing the energies and wave functions of the solid by those of the octahedral cluster. If
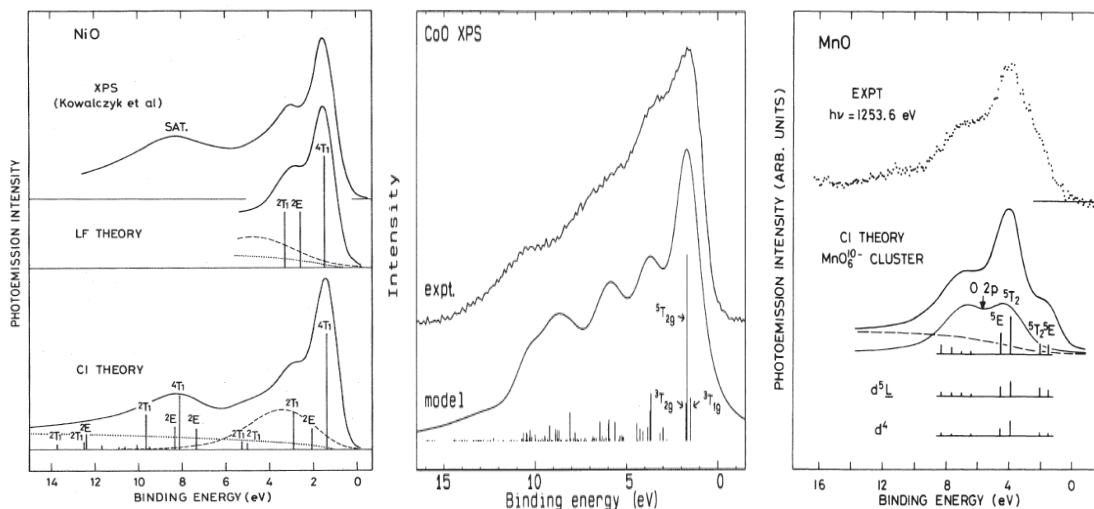
Fig. 4: *Comparison of experimental valence band photoemission spectra and results from cluster calculations: NiO (left), CoO(center), MnO(right). Reprinted with permission from [19], Copyright 1984 by the American Physical society, from [20], Copyright 1991 by the American Physical society, and from [21], Copyright 1990 by the American Physical society.*

we moreover let $T \to 0$ the sum over μ becomes a sum over the m degenerate ground states of the cluster and $e^{-\beta E_\mu}/Z \to 1/m$. The underlying assumption is that the coupling of the clusters to its environment in the solid will predominantly broaden the ionization states of the cluster into bands of not too large bandwidth. This broadening is usually simulated by replacing the δ-functions by Lorentzians. To compare to a measured spectrum, the calculated spectrum often is convoluted with a Gaussian to simulate the finite energy resolution of the photoelectron detector.

Figure 4 shows various examples from the literature where measured XPS-spectra are compared to spectra calculated by the procedure outlined above. The sticks in some of the theoretical spectra mark the final state energies E_ν and are labeled by the symbols of the irreducible representation of the octahedral group to which the corresponding final state wave function $|\Psi_\nu\rangle$ belongs. The figure shows that the agreement between the theoretical spectra and experiment is usually rather good. It is interesting to note that the three oxides shown in the figure all have the same crystal structure, namely the rocksalt structure. Since moreover Ni, Co and Mn are close neighbors in the periodic table, LDA predicts almost identical band structures with the main difference being an upward shift of the chemical potential with increasing nuclear charge of the transition metal. Despite this, the XPS spectra differ considerably and this change is reproduced very well by the theoretical spectra. This is clear evidence that the shape of the spectra is determined not so much by the single particle band structure, but by the multiplet structure of the transition-metal ion, which in turn depends on its valence and spin state.

How then does the multiplet structure determine the photoelectron spectrum? As mentioned above, if we neglect charge transfer, photoemission corresponds to the transition from the ground state of d^n, i.e. the lowest state in the Tanabe-Sugano diagram for the respective n, to some eigenstate of d^{n-1}. This final state, however, is nothing but some state in the Tanabe-

Sugano diagram for d^{n-1}. Moreover, if the ground state of d^n has spin S, the final state must have spin $S \pm \frac{1}{2}$ so that the number of possible final states is significantly restricted. In this way, the photoemission spectrum will contain relatively few sharp lines whose positions are determined by the energies of the multiplets.

Next, we discuss X-ray absorption. In an X-ray absorption experiment an electron from either the $2p$- or the $3p$-shell absorbs an incoming X-ray photon and is promoted to the $3d$-shell via a dipole transition. In terms of electron configurations, the transition thus is $2p^6 3d^n \rightarrow 2p^5 3d^{n+1}$ (for definiteness we will always talk about the $2p$-shell from now on). Of particular interest here is the range of photon energies just above the threshold were the energy of the photon is sufficient to lift the core electron to an unoccupied state. Above this threshold the X-ray absorption coefficient $\kappa(\omega)$ rises sharply, which is called an absorption edge. The energy of the edge thereby is characteristic for a given element so that one can determine unambiguously which atom in a complex solid or molecule is probed. The ω-dependence of $\kappa(\omega)$ in an energy range of a few eV above the absorption edge, called NEXAFS for Near Edge X-ray Absorption Fine Structure, contains information about the initial state of the $3d$-shell, i.e., its valence and spin state, and this information can be extracted by using cluster calculations. The measured quantity in this case is

$$
\begin{aligned}
\kappa(\omega) &= -\frac{1}{\pi Z} \Im \sum_{m=-2}^{2} \sum_{\mu} e^{-\beta E_\mu} \left\langle \Psi_\mu \left| D(\boldsymbol{n}) \frac{1}{\omega - (H - E_\mu) + i0^+} D(\boldsymbol{n}) \right| \Psi_\mu \right\rangle \\
&= \frac{1}{Z} \sum_{m=-2}^{2} \sum_{\mu,\nu} e^{-\beta E_\mu} |\langle \Psi_\nu | D(\boldsymbol{n}) | \Psi_\mu \rangle|^2 \, \delta(\omega - (E_\nu - E_\mu)).
\end{aligned}
\tag{19}
$$

This is very similar to the single-particle spectral function (18), the only difference is that now the dipole operator $D(\boldsymbol{n})$ appears in place of the electron annihilation operator $c_{3,2,m,\sigma}$. This also implies that the number of electrons in the final states $|\Psi_\nu\rangle$ now is equal to that in the initial states $|\Psi_\mu\rangle$.

We again make the approximation to use the octahedral cluster to simulate this experiment. The initial state for this experiment, $2p^6 3d^n$, is simply the ground state of the cluster. More difficult is the final state, $2p^5 3d^{n+1}$. This has a hole in the $2p$-shell so that the single-particle basis has to be enlarged once more to comprise also the 6 spin-orbitals available for $2p$ electrons. We may restrict the basis, however, to include only states with 5 electrons (or 1 hole) in these 6 spin-orbitals, so that the dimension of the Hilbert space increases only by a moderate factor of 6. The spin-orbit coupling constant $J_{SO,2p}$ in the $2p$-shell of $3d$ transition-metals is of order 10 eV so we definitely need to include spin-orbit coupling in the $2p$-shell. Here the forms (13) and (14) with $l = 1$ can be used. The orbital angular momentum $l = 1$ and the spin of $\frac{1}{2}$ can be coupled to a total angular momentum of either $J = \frac{3}{2}$ or $J = \frac{1}{2}$. Using the identity

$$
\langle \boldsymbol{L} \cdot \boldsymbol{S} \rangle = \frac{1}{2} \Big(J(J+1) - L(L+1) - S(S+1) \Big)
$$

we expect a splitting of $E_{\frac{3}{2}} - E_{\frac{1}{2}} = \frac{\lambda_{SO}}{2}(\frac{15}{4} - \frac{3}{4}) = \frac{3\lambda_{SO}}{2}$. This means that we actually have two edges, separated by $\frac{3\lambda_{SO}}{2} \approx 10 - 15$ eV for $2p$ core levels. The one for lower photon energy,
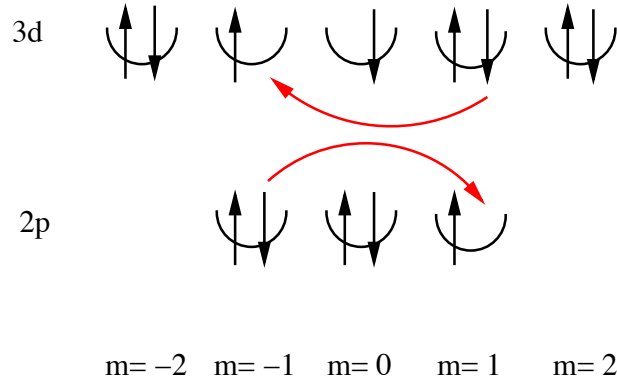
3d

2p

m= −2   m= −1   m= 0   m= 1   m= 2

Fig. 5: *An electron in the $3d$-shell and an electron in the $2p$-shell scatter from one another.*

called the L_3 edge, is due to electrons coming from $^2P_{3/2}$, the one for higher photon energy (L_2-edge) due to electrons from $^2P_{1/2}$. Since there are 4 $^2P_{3/2}$ states but only 2 $^2P_{1/2}$ states the L_3 edge has roughly twice the intensity of the L_2 edge.

Next, there is the Coulomb interaction between the core-hole and the electrons in the d-shell. For example, there may now be Coulomb scattering between a $2p$ and a $3d$ electron as shown in Figure 5.

This, however, is again described by the corresponding Coulomb matrix element (9). Here now one of the indices ν_1 and ν_2 and one of the indices ν_3 and ν_4 must refer to the $2p$-orbital and there are two possible combinations. If ν_2 and ν_3 refer to the $2p$-orbital we have

$$\sum_k c^k(2, m_1; 2, m_4)\, c^k(1, m_3; 1, m_2)\, F^k(3, 2; 2, 1).$$

The triangular condition for $c^k(1, m_3; 1, m_2)$ requires $k \le 2$. Since only Y_{lm} with equal l and hence with equal parity are combined in one c^k only even k give nonvanishing contributions and we have two relevant Coulomb integrals, $F^0(2, 3; 2, 1)$ and $F^2(2, 3; 2, 1)$.

If ν_2 and ν_4 refer to the $2p$-orbital we have

$$\sum_k c^k(2, m_1; 1, m_4)\, c^k(2, m_3; 1, m_2) G^k(3, 2; 2, 1).$$

The triangular condition for both c^k requires $k \le 3$. Since now Y_{1m} and Y_{2m} are combined in one Gaunt coefficient only odd k contribute, so that we have two relevant exchange integrals, $G^1(3, 2; 2, 1)$ and $G^3(3, 2; 2, 1)$. Apart from these minor changes, the implementation of the d-p Coulomb interaction is exactly the same as for the d-d interaction.

The Coulomb interaction between electrons in the $2p$-shell is definitely very strong, but it is irrelevant because we are considering only states with a *single hole* in this shell. Since this hole has no second hole to scatter from, the only effect of the Coulomb repulsion between electrons in the $2p$-shell is via the diagonal matrix elements which give a shift of the orbitals energy ϵ_{2p}. On the other hand ϵ_{2p} merely enters the position of the absorption edge, which would be $\approx \epsilon_{3d} - \epsilon_{2p}$, but not its spectral shape. Since we are not really interested in computing the onset of the edge, the precise value of ϵ_{2p} and hence the Coulomb interaction between $2p$ electrons is not important. The CEF effect on the inner shell electrons is usually neglected.
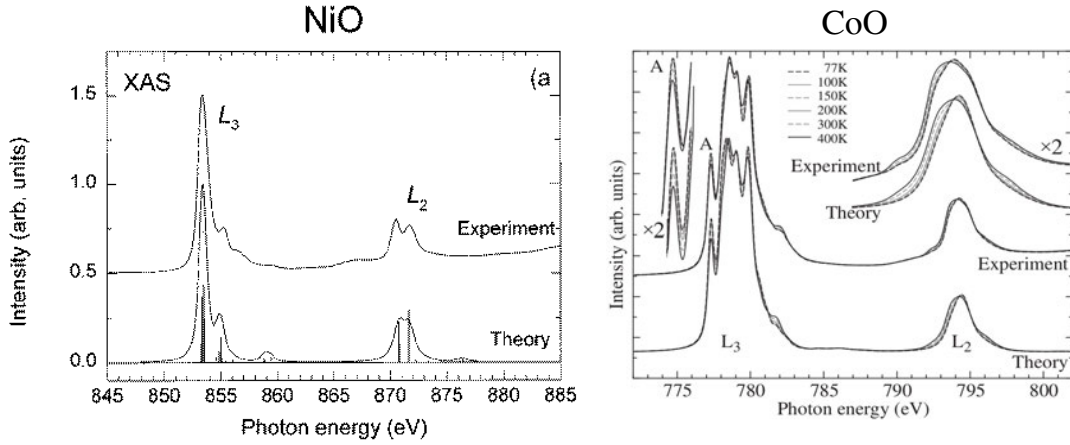
Fig. 6: *Comparison of experimental 2p XAS-spectra and results from cluster calculations: NiO (left) and CoO (right). Reprinted with permission from [22], Copyright 1999 by the American Physical society, and with permission from [23].*

Lastly, we discuss the dipole operator $D(\boldsymbol{n})$. This involves the matrix element of $\boldsymbol{n} \cdot \boldsymbol{r}$, where $\boldsymbol{n}$ is the vector which gives the polarization of the X-rays. This can be rewritten as

$$\boldsymbol{n} \cdot \boldsymbol{r} = r \sqrt{\frac{4\pi}{3}} \sum_{m=-1}^{1} \tilde{n}_m \, Y_{1,m}(\vartheta, \varphi) \,,$$

where $\tilde{n}_1 = (-n_x + in_y)/\sqrt{2}$, $\tilde{n}_0 = n_z$ and $\tilde{n}_{-1} = (n_x + in_y)/\sqrt{2}$. It follows that

$$O(\boldsymbol{n}) = \sum_{m,m'} \sum_{\sigma} d_{m,m'} \, c^{\dagger}_{3,2,m,\sigma} \, c_{2,1,m',\sigma}$$

$$d_{m,m'}(\boldsymbol{n}) = d \, \tilde{n}_{m-m'} \, c^1(2,m;1,m')$$

$$d = \int_0^{\infty} dr \, r^3 \, R_{3,2}(r) \, R_{2,1}(r) \,.$$

The factor of d merely scales the overall intensity of the spectrum and is largely irrelevant. Combining all of the above one can compute X-ray absorption spectra. Figure 6 shows examples from the literature where experimental $2p$-XAS spectra for NiO and CoO are compared to spectra obtained from the cluster model described above. In both cases one can see the splitting of approximately 15 eV between the L_3 and L_2 edges. The edges have an appreciable fine structure, however, which is reproduced well by theory. The spectrum for CoO is shown at different temperatures and indeed has a significant temperature dependence. The origin of the temperature dependence is as follows: Cobalt is Co^{2+} or d^7 in CoO and the ground state of d^7 in cubic symmetry is a spin quartet and is orbitally three-fold degenerate so that the total degeneracy is $n = 12$. In this situation, the weak spin-orbit interaction in the $3d$-shell can lift the 12-fold degeneracy and produce several closely spaced eigenstates. The splitting between these 12 eigenstates is of the order of the spin-orbit coupling constant in the $3d$-shell, $\lambda_{SO} \approx 50$ meV, and the higher lying states therefore may be thermally populated with increasing temperature (see the Boltzmann factors in (19)). This leads to the temperature dependence of the spectra which obviously is reproduced at least qualitatively by the cluster calculation.

XPS and XAS experiments are often performed because for example the valence or the spin state of the transition-metal ion in a given solid or molecule is unknown. Let us assume that we have two possible states of the ion, $|\Psi_0\rangle$ and $|\Psi_0'\rangle$, with energies E_0 and E_0' (for simplicity we assume that these are nondegenerate). Then we may ask: how will the spectrum change if we go from one ground state to the another? We note first that the final states $|\Psi_\nu\rangle$ and their energies E_ν in (18) and (19) are unchanged. What differs is first the energy differences $E_\nu - E_0$. However, since we do not know E_0 and E_0', otherwise we would know which one of them is lower in energy and hence the ground state, the absolute position of the peaks in the spectrum is of no significance. What is really relevant is the *intensity* of the peaks which involves the matrix elements $|\langle\Psi_\nu|c|\Psi_0\rangle|^2$ or $|\langle\Psi_\nu|D(\boldsymbol{n})|\Psi_0\rangle|^2$. These matrix elements may change drastically when the ground state wave function $|\Psi_0\rangle$ changes and by comparing with cluster simulations the shape of the spectrum can give information about the valence and spin state of the transition-metal ion.

To summarize this section: multiplet theory is of considerable importance in the interpretation of photoelectron spectroscopy and X-ray absorption. The simulated spectra usually show very good agreement with experimental ones. All of this shows that the multiplets of the free ion persist in the solid and that the proper description of the Coulomb interaction is crucial for the description of these compounds.

5   Conclusion

We have seen that the Coulomb repulsion between electrons in partially filled atomic shells leads to multiplet splitting. The multiplets may be viewed as collective excitations of the 'not-so-many-body-system' formed by the electrons in a partially filled atomic shell. We have seen that a relatively simple theory, essentially degenerate first order perturbation theory, describes the energies of the multiplets quite well and gives a good description of the line spectra of free atoms. When transition-metal atoms are embedded into a solid, the collective excitations of the electrons in their partly filled $3d$-shells are modified by the crystalline electric field of their environment and by hybridization with orbitals on neighboring atoms. If these effects are taken into account, which is relatively easy if one uses exact diagonalization, the resulting 'extended multiplet theory' turns out to be spectacularly successful in reproducing a wide variety of experimental results for transition-metal compounds. Photoemission spectra, X-ray absorption spectra, optical absorption spectra, electron spin resonance, and inelastic neutron scattering can be interpreted in terms of multiplet theory. The often excellent agreement between theory and experiment which can be thereby obtained is clear evidence that the multiplets of the free ion are a reality also in solids, with the only modification being some additional splitting due to the lowering of the symmetry and the modification of spectral intensities due to charge transfer. It has to be kept in mind, however, that in order to obtain agreement with experiment it is crucial to use the full Coulomb Hamiltonian, with its matrix elements expressed in terms of Slater-Condon parameters and Gaunt coefficients. Put another way, we may summarize the present lecture in three words: Multiplets do matter!

A   Gaunt coefficients

m	m'	c^0	$7\,c^2$	$21\,c^4$	a^0	$49\,a^2$	$441\,a^4$	b^0	$49\,b^2$	$441\,b^4$
± 2	± 2	1	-2	1	1	4	1	1	4	1
± 2	± 1	0	$\sqrt{6}$	$-\sqrt{5}$	1	-2	-4	0	6	5
± 2	0	0	-2	$\sqrt{15}$	1	-4	6	0	4	15
± 1	± 1	1	1	-4	1	1	16	1	1	16
± 1	0	0	1	$\sqrt{30}$	1	2	-24	0	1	30
0	0	1	2	6	1	4	26	1	4	36
± 2	∓ 2	0	0	$\sqrt{70}$	1	4	1	0	0	70
± 2	∓ 1	0	0	$-\sqrt{35}$	1	-2	-4	0	0	35
± 1	∓ 1	0	$-\sqrt{6}$	$-\sqrt{40}$	1	1	16	0	6	40

Table 5: *The Gaunt coefficients $c^k(2, m; 2, m')$ and the products $a^k(2, m; 2, m')$ and $b^k(2, m; 2, m')$*

References

[1] J.H. de Boer and E.J.W. Verwey, Proc. Phys. Soc. London 49, 59 (1937)

[2] Yu. Ralchenko, A.E. Kramida, J. Reader, and NIST ASD Team (2011)
NIST Atomic Spectra Database (ver. 4.1.0): `http://physics.nist.gov/asd`

[3] L.D. Landau and E.M. Lifshitz: *Course of Theoretical Physics*
(Pergamon Press, Oxford New York, 1977)

[4] A.L. Fetter and J.D. Walecka: *Quantum Theory of Many Particle Systems*
(McGraw-Hill, San Francisco, 1971)

[5] J.C. Slater: *Quantum Theory of Atomic Structure*
(McGraw-Hill, New York, 1960)

[6] J.S. Griffith: *The Theory of Transition Metal Ions*
(Cambridge University Press, Cambridge, 1961)

[7] V.I. Anisimov, I.V. Solovyev, M.A. Korotin, M.T. Czyzyk, and G.A. Sawatzky,
Phys. Rev. B **48** (1993)

[8] J. Kunes, V.I. Anisimov, A.V. Lukoyanov, and D. Vollhardt
Phys. Rev. B **75**, 165115 (2007)

[9] B.N. Figgis: *Introduction to Ligand Fields*
(Interscience Publishers, New York London Sydney, 1966)

[10] S. Sugano, Y. Tanabe, and H. Kitamura: *Multiplets of Transition Metal Ions*
(Academic Press, New York 1970)

[11] M. Foulkes, lecture at this school

[12] E. Koch in *Many-Body Physics: From Kondo to Hubbard*
Reihe Modeling and Simulation, Vol. 5 (Forschungszentrum Jülich, 2015)
`http://www.cond-mat.de/events/correl15`

[13] See e.g. the CTM4XAS package:
`http://www.anorg.chem.uu.nl/CTM4XAS/index.html`

[14] F.M.F. de Groot, Journal of Electron Spectroscopy and Related Phenomena, **67** 525 (1994)

[15] F.M.F. de Groot, Coordination Chemistry Reviews, **249** 31 (2005)

[16] F.M.F. de Groot and A. Kotani: *Core Level Spectroscopy of Solids*
(Taylor And Francis, Abingdon on Thames, 2008)

[17] C. Caroli, D. Lederer-Rozenblatt, B. Roulet, and D. Saint-James,
Phys. Rev. B **8**, 4552 (1973)

[18] P.J. Feibelman and D.E. Eastman, Phys. Rev. B **10**, 4932 (1974)

[19] A. Fujimori and F. Minami, Phys. Rev. B **30**, 957 (1984)

[20] J. van Elp, J.L. Wieland, H. Eskes, P. Kuiper, G.A. Sawatzky, F.M.F. de Groot, and
T.S. Turner, Phys. Rev. B **44**, 6090 (1991)

[21] A. Fujimori, N. Kimizuka, T. Akahane, T. Chiba, S. Kimura, F. Minami, K. Siratori,
M. Taniguchi, S. Ogawa, and S. Suga, Phys. Rev. B **42**, 7580 (1990)

[22] M. Finazzi, N.B. Brookes, and F.M.F. de Groot, Phys. Rev. B **59**, 9933 (1999)

[23] M. Haverkort, PhD Thesis (Universität zu Köln, 2005, see also arXiv:cond-mat/0505214)